TECHNICAL MEMORANDUMS

NATIONAL ADVISORY COMMITTEE FOR AERONAUTICS

No. 343

POTENTIAL FLOW IN ENGINE VALVES

By Bruno Eck

Reprint from "Zeitschrift für angewandte Mathematik und Mechanik," Vol. IV, 1924.

Washington
December, 1925

NATIONAL ADVISORY COMMITTEE FOR AERONAUTICS.

TECHNICAL MEMORANDUM NO. 343.

POTENTIAL FLOW IN ENGINE VALVES.*

By Bruno Eck.

The extensive applicability of the hydrodynamic theory to the problems of engine construction is clearly shown in the following attempt to determine by exact methods the nature of the flow in valves under variously restricted conditions. Observation shows that two principal kinds of flow occur in simple flat-seated valves. For small valve lifts, the flow is along the horizontal wall and is therefore deflected 90°, but for greater valve lifts the flow separates and forms a free stream, whose angle of deflection naturally increases with increasing lift. Both these kinds of flow can, in fact, be theoretically explained.

In order to simplify the flow and render computation possible, the following measures are adopted:

1. The whole problem is treated two-dimensionally;

2. The effect of friction is disregarded;

3. It is assumed that the fluid, after leaving the valve opening, forms a free stream, which extends into infinity at an angle α, notwithstanding the fact that the space over the valve head is mostly filled with the same fluid and that

* Contribution from the Aerodynamic Institute of the Aachen Technical High School, reprinted from "Zeitschrift für angewandte Mathematik und Mechanik," Vol. IV, 1924, pp. 464-474.

the fixed walls very quickly set limits to the formation of the stream.

The theory of discontinuity surfaces evolved by Kirchhoff and Helmholtz is preferably employed for the solution of two-dimensional problems of this kind. This theory does not require constancy of velocity at the points where the ordinary theory would require a very high velocity, namely, near the sharp corners of the body. The very great velocity would, according to Bernouilli's equation, demand a very great negative pressure at these points, which is probably not assumable from the physical viewpoint for ordinary fluids. Therefore, in order to harmonize such a solution with the reality, we can assume that these points are shut out from the flow by a small circle, or that any slight rounding would necessitate very great but not infinitely great velocities. Kirchhoff stated the mathematical methods for the convenient application of this theory to similar special cases. These methods consist chiefly in finding the conformable diagram of the hodograph on the plane of the velocity potential, which is always successful when the rigid walls are flat.

1. Stream free on both sides.- We will first consider a flow (Fig. 1), which, coming from infinity (A), is confined by the parallel walls AB and AE, breaks off at C and E, forms a free surface and then extends to infinity at an angle α. The stream is assumed to be confined by a free surface, i.e.,

the velocity on the boundary is assumed to fall discontinuously to zero.* If there is a pressure p_o in the still fluid, it follows from Bernouilli's equation that the velocity is constant on the free surface. If we put this velocity = 1, it denotes no specialization, but only a simplification of the calculation, which can be offset by a suitable disposition of the mass units. From C, through $D = \infty$, up to E, the velocity is therefore 1, while from the point B, the pressure increases from 0 to 1.

If the potential function of the flow sought is designated by $x = \varphi + i\psi$, then $dx/dz = u - iv = w$ represents the velocity, the direction of the motion being reflected on the x axis.

Since w for the margin of the flow is known partly by the absolute magnitude and partly by the direction, we can determine the limits of the w plane (Fig. 2). At B, $w = 0$ and at C the free surface begins (i.e., $w = 1$), so that the limits of the free surface must lie on the unit circle and de-

* You are here referred to the valuable works of Sir G. Greenhill, British Advisory Committee for Aeronautics, No. 19, 1910, "Theory of a Streamline Past a Plane Carrier and of the Discontinuity Arising at the Edge," which gives quite a complete list of all the kinds of flow occurring in this field, along with their diagrammatic treatment.

R. von Mises ("Zeitschrift des Vereines Deutscher Ingenieure," 1917, pp. 447 ff, "Berechnung von Ausfall und Ueberfallzahlen") had previously discussed this problem thoroughly and had in fact, calculated the coefficients for the form of flow here considered.

scribes the quadrant from C to E. From E to A, $u = 0$ and v falls from 1 to a certain value κ which we will provisionally assume to be less than 1. From A to B, $u = 0$, so that the whole flow in the w plane is portrayed by a quadrant.

The connection between $x = \varphi + i\psi$ and $w = u - iv$ follows from $dx/dz = w$. This is a complex differential equation, the solution of which is decisive for our problem. In our solution, we find $x = fz$ and utilize the differential equation for finding this expression, by first obtaining $x = g\,w$ and then finding $z = \int \frac{dx}{w}$ by an integration. An expression for the function x, similar to the one for w, is indeed known, since its limits can also be given. In the theory of functions, the conformable diagram affords a convenient method for finding $x = g\,w$.

For the further calculation, it is more convenient to work with the natural logarithm of w instead of with w itself, a simplification also employed in the cases subsequently treated (Fig. 3).

The further calculation is as follows. The strip BCEAB is plotted on a half-plane, so that the boundary falls on the real axis. The same thing happens with the potential plane x. These half-planes are then so superposed that the corresponding points coincide, by which operation the function $x = g\,w$ is found.

The plotting of BCEA on the half-plane (Fig. 4) is accomplished by means of Christoffel's integral

$$w' = w + i\frac{\pi}{4} = C' \int \frac{dz'}{\sqrt{z'^2 - \zeta_o^2}} + B',$$

an assertion which can be easily verified by remembering that

$$\text{arc}\,\frac{dw'}{dz'} = \frac{1}{(z' + \zeta_o)^{1/2}\,(z' - \zeta_o)^{1/2}}$$

is increased by $\pi/2$ at the points $\pm\zeta_o$. After determining the constants, we obtain

$$z' = \zeta_o^{1/2}\,\frac{w^4 + 1}{w^2}.$$

Plotting the potential on the half-plane.- The boundary lines ABCD and AED form streamlines between which the whole stream flows (Fig. 5). The potential is thus plotted on a strip $\psi_B - \psi_E$. This difference is, at the same time, the amount of the fluid flowing through. In order to have a definite case in mind, we put $\psi_B - \psi_E = \pi$. By means of $z = e^{\varphi + i\psi}$ this strip is plotted on the half-plane, so that $z = B$ comes after -1, A comes after 0 and D remains in infinity.

If we now establish, by a linear transformation, a connection between the two half-planes, so that corresponding points coincide, we obtain the function $x = f\,w$. In the expression $z = \frac{z' + a}{z'b + c}$, we determine the constants a, b, c, so that $z' = B$ after $\pm\infty$ and $z' = A = -\zeta_o^{1/2}\,(\kappa^2 + \frac{1}{\kappa^2})$ after $z = 0$ and thus obtain

$$z = \frac{z' + \zeta_0 \frac{\kappa^4 + 1}{\kappa^2}}{-z' + c},$$

or with the insertion of $\lambda = \frac{\kappa^4 + 1}{\kappa^2}$ and $-2\frac{c}{\zeta_0} = \mu$

$$z = -\frac{w^4 + \lambda w^2 + 1}{w^4 + \mu w^2 + 1} \quad \text{or, since} \quad z = e^{\varphi + i\psi},$$

$$\psi + i\psi = \log \frac{w^4 + \lambda w^2 + 1}{w^4 + \mu w^2 + 1} \tag{1}$$

The importance of μ is due to the fact that the points $\varphi + i\psi = \pm\infty$ must have known velocity values. With this condition, we find that $\mu = -2 \cos 2\alpha$, in which α is the angle formed by the stream in infinity with the x axis.

The parameters occurring in the solution, with which we can satisfy the prescribed geometric conditions of flow, are especially important. It is obvious that they must be connected with the physical properties of the flow. It is in fact apparent from equation (1) that only the two following parameters occur:

1. The ratio of the velocities at A and D equals κ;

2. The angle α, which the stream in infinity forms with the x axis.

Since the three quantities b, h and r = BC must be determined, only the relations $n = h/b$ and $m = r/b - 1$, obtained by two integrations, can be involved. The relation between w and x is established through equation (1). From $\frac{dx}{dz} = w$ it follows that $dz = \frac{dx}{w}$ and $z = \int \frac{dx}{dw}\,\frac{dw}{w}$, which is simpli-

fied by the elimination of dx, since dx/dw is known.

$$z = \int_{w_1}^{w_2} \frac{4w^2 + 2\lambda}{w^4 + \lambda w^2 + 1}\, dw - \int_{w_1}^{w_2} \frac{4w^2 + 2\mu}{w^4 + \mu w^2 + 1} \qquad (2)$$

Zero and unity are the integration limits for r and h. We obtain

$$r = 2\frac{\kappa^2 - 1}{\kappa} \arctan\kappa + \frac{\pi}{\kappa} + \cos\alpha \log\frac{1 + \cos\alpha}{1 - \cos\alpha} - \pi\sin\alpha,$$

$$h = i\frac{\kappa^2 + 1}{\kappa} \log\frac{1 + \kappa}{1 - \kappa} + \frac{\pi}{\kappa} + i\pi\cos\alpha - 1\sin\alpha \log\frac{1 + \sin\alpha}{1 - \sin\alpha}.$$

For the relations $m = \frac{r}{b} - 1$ and $n = \frac{h}{b}$, we obtain, by taking into consideration for $h_o = b + i\,h$ only the imaginary component

$$m = -2\frac{1 - \kappa^2}{\pi} \arctan\kappa + \kappa\left\{\frac{\cos\alpha}{\pi} \log\frac{1 + \cos\alpha}{1 - \cos\alpha} - \sin\alpha\right\} \qquad (3)$$

$$n = \frac{1 + \kappa^2}{\pi} \log\frac{1 + \kappa}{1 - \kappa} + \kappa\left\{\cos\alpha - \frac{\sin\alpha}{\pi} \log\frac{1 + \sin\alpha}{1 - \sin\alpha}\right\} \qquad (4)$$

Equations (3) and (4) represent the solution of the first problem. They always go together, so that here we have a set of equations with three unknown quantities. If, for example, an overlapping m is stipulated, m must be introduced into equation (3), then the values of κ and α which satisfy equation (3) must be determined and then these values must be introduced into equation (4), from which we obtain the valve-lift n. This procedure must be followed for all values of α which satisfy equation (3).

Such a computation would be very tedious and the determi-

nation of the relations for any desired variation of m would mean much work. It was therefore a great advantage that the special form of equations (3) and (4) (which could be written in the form $m = - f_1 \kappa + \kappa g_1 \alpha$ and $n = f_2 \kappa + \kappa g_2 \alpha$) allowed the employment of nomographic methods, by means of which it was possible to find the corresponding κ, α and n for m from 0 to ∞ which were then combined in the following manner.

a) Velocity plotted against the valve-lift.- $n = f \kappa$ (Fig. 6). κ increases almost linearly at first and, with increasing n, approaches asymptotically the value 1. It is noticeable that all the curves m = const. lie very close together, so that any change in the overlapping has but little effect on the velocity. For the valve-lifts occurring in practice up to n = 1, the n curve closely approximates a straight line.

b) $\alpha = g \kappa$ (Fig. 7).- The overlapping has, as was to be expected, a greater effect on α. For small values of m, α increases with relative rapidity and tends toward a limit, as n increases. This limit falls for larger values of m, so that at $m = \infty$ only $\alpha = 0$ is possible. It is noteworthy that, with positive overlappings, the maximum attainable angle is 36°.

c) Coefficient of contraction (Fig. 8).- It can be readily shown that a criterion for the contraction of the emergent stream is given by $\mu = \frac{\delta}{n}$, when δ denotes the thickness of the stream. The course of these values indicates a very slight

dependence on m. For very small values of κ, α is found, by computing the limiting value for m, to have the value $\frac{\pi}{\pi + 2}$. This is then manifestly identical with Kirchhoff's case of the flow from an infinitely long slit.

d) The pressure-loss coefficient $\zeta = \frac{1 - \kappa^2}{\kappa^2}$ was also plotted (Fig. 9). Its curves are very slightly affected by m and are strongly hyperbolic.

2. Stream free on only one side.- For very small valve-lifts, as mentioned in the introduction, the experiments showed a flow, which did not separate at the point E, but was deflected 90° (Fig. 10). It was found that, even mathematically, such a flow exists, which is treated in what follows. The free surface is assumed to begin at C, whose angle α' with the x axis increases to a maximum value α at the point F and then again in infinity attains the value $\alpha' = 0$. The question here is not therefore concerning an entirely free stream, but concerning a stream which is bounded on one side by a fixed wall and on the other by a free surface.

The interesting problem now arises as to whether all conditions of flow, which can occur physically in a configuration like the flat valve have already been exhausted in the foregoing cases. It is, in fact, possible to carry out an investigation of this kind, which bears principally on the subject of the log w plane. The hereby mathematically possible cases are not always physically possible.

If we obtain, for example, a margin of the log w plane, where the limits have no neighboring infinite streamlines, then this naturally has no further physical significance, even though it may still be of some interest as a theoretical function. Without continuing this discussion, it may be mentioned that only one other flow is possible in the above case (Fig. 11). Here also the stream bends 90° at E and follows the horizontal wall, which it leaves, however, at E' where the free surface begins. The angle α' then gradually increases until it reaches its maximum at $D = \infty$. On the other side, the angle decreases until it reaches the value $\alpha = 0$ at C. The mathematical treatment of the last two cases is very similar and they will therefore be considered side by side. For the purpose of distinguishing them, the first will be designated by IIa, and the second by IIb. The principle of the calculation is essentially covered in Section 1, although the difficulties are much greater here. It is easily seen that the velocity range of IIa and IIb is represented by a "quarter-plane" (Fig. 12), which is cut along the unit circle from C to F and back to D. The angle CBF is the maximum angle α. The log w plane is obtained in a corresponding manner (Fig. 13). The difference between IIa and IIb consists in the fact that several conspicuous points are shifted, a circumstance which is first manifested by the diagram of the potential half-plane on the velocity-potential plane. The diagram of the log w plane on the half-plane might even here be accomplished by the Chris-

toffel integral, but the purely formal difficulties are considerably greater than by the following method. The problem can here be more conveniently solved by three auxiliary diagrams, which successively show the log w strips on a slotted half-plane and on an unslotted half-plane.

The strip of the log w plane on a half-plane is represented by $z = \sqrt{1 + \frac{\sin^2 \omega}{\sin^2 \alpha}}$, which is cut out along the imaginary axis from $\frac{i}{\tan\alpha}$ to ∞ (Fig. 14). A reflection on the unit circle $z = \frac{1}{\zeta}$ shifts the slot from ∞ to 0 and from $\frac{i}{\tan\alpha}$ to $-i \tan\alpha$ (Fig. 15). The half-plane slotted from 0 to $-i \tan\alpha$ is finally depicted on the half-plane (Fig. 16) by the third diagram $\zeta^2 = \tan^2\alpha\,(f^2 - 1)$. On eliminating the individual steps, we find, for the diagram of log w plane on the half plane, the function

$$f^2 = \frac{\cos^2 \omega}{\cos^2\omega - \cos^2\alpha} = \frac{\cos^2(\log w)}{\cos^2(\log w) - \cos^2\alpha}$$

The potential planes depicted on the half-plane by $s_1 = e^{X_1}$ or $s_2 = e^{X_2}$ are covered by a linear transformation, so that every three corresponding points coincide. The expressions $s_1 = \ldots$ and $s_2 = \ldots$ $\zeta_1 = \frac{f + a_1}{fc_1 + b_1}$ and $\frac{f + a_2}{fc_2 + b_2}$ lead (after determining the constants and eliminating the individual auxiliary variables) to the equations

$$e^{X_1} = \tau \frac{\frac{\cos(\log w)}{\sqrt{\cos^2(\log w) - \cos^2\alpha}} + \frac{1 - \kappa^2}{\sqrt{(1 - \kappa^2)^2 + 4\kappa^2 \cos^2\alpha}}}{\frac{\cos(\log w)}{\sqrt{\cos^2(\log w) - \cos^2\alpha}} - \frac{1}{\sin\alpha}} \qquad (5)$$

$$e^{X_2} = \mu \left\{ \frac{\cos (\log w)}{\sqrt{\cos^2 (\log w) - \cos^2\alpha}} + \frac{1 - \kappa^2}{\sqrt{(1 - \kappa^2)^2 + 4\kappa^2 \cos^2\alpha}} \right\} \quad (6)$$

The statements in section 1 concerning parameters apply here unchanged, since only κ and α occur, with which the dimensions can be determined again. In particular the integrals $z = \int \frac{dx}{\omega}$ must be again calculated here. The very difficult determination of these integrals was made possible by the choice of the f plane for the integration

$$z = \int \frac{dx}{w} = \int \frac{1}{w} \frac{dx}{df} df = \int e^{-\omega} \frac{dx}{df} df,$$

since $w = e^{i\omega}$.

Flow IIa: $$z = \int \left\{ \frac{f \cos\alpha}{\sqrt{f^2-1}} \sqrt{\frac{1 - f^2\sin^2\alpha}{f^2 - 1}} \right\} \left\{ \frac{1}{\overline{f} + fa} - \frac{1}{f - \frac{1}{\sin\alpha}} \right\} df,$$

Flow IIb: $$z = \int \left\{ \frac{f \cos\alpha}{\sqrt{f^2-1}} - \sqrt{\frac{1 - f^2\sin^2\alpha}{f^2 - 1}} \right\} \frac{1}{f + \overline{f}a} df.$$

It is obvious that the integrals are composed of elementary components and elliptical integrals of the first, second and third kinds. We will not go farther into the very troublesome calculations and will only give the result.

$$m = \frac{\kappa}{\pi}\cos\alpha\,\log\left(\operatorname{cotan}\frac{\alpha}{2}\right) - \frac{1-\kappa^2}{2\pi}\arccos\frac{fa-\sin\alpha}{1-fa\,\sin\alpha} - \frac{\kappa}{2}\sin\alpha - \frac{1}{2(1+\cos\theta)}$$

$$+ \frac{\kappa\,fa}{\pi\sin\theta\,\cos\theta}\left\{\frac{\pi}{2} + (F-E)\,(F(\theta,k') - F\,E(\theta,k')\right\}$$

$$\underline{- \frac{\kappa}{2}\cos\alpha\,\log\left(\operatorname{cotan}\frac{\alpha}{2}\right) + \frac{\kappa}{\pi}\log\frac{1}{\sin\alpha} - \frac{\kappa}{\pi}\sin\alpha\left(F - \frac{\pi}{2}\right)}$$

$$n = \kappa\cos\alpha + \frac{1+\kappa^2}{\pi}\left\{\overline{F}\,\overline{E}(\Gamma) - \overline{E}\,\overline{F}(\Gamma)\right\} - \underline{\frac{\kappa\cos\alpha + \kappa - \frac{2\kappa}{\pi}\sin\alpha\,F}{}} \qquad (7)$$

All the equations apply to the flow IIa and the equation without underlined terms applies also to IIb. The individual constants have the following values:

$$fa = \frac{1-\kappa^2}{\sqrt{(1-\kappa)^2 + 4\kappa^2\cos^2\alpha}}; \quad \tan\frac{\theta}{2} = \kappa; \quad F = \int_0^{\pi/2}\frac{d\varphi}{\sqrt{1-\cos^2\alpha\,\sin^2\varphi}};$$

$$E = \int_0^{\pi/2}\sqrt{1-\cos^2\alpha\,\sin^2\varphi}\,d\varphi$$

$$F(\theta,k') \int_0^{\theta}\frac{d\varphi}{\sqrt{1-\cos^2\alpha\,\sin^2\varphi}}; \quad E(\theta,k') = \int_0^{\theta}\sqrt{1-\cos^2\alpha\,\sin^2\varphi}\,d\varphi$$

$$\overline{F} = \int_0^{\pi/2}\frac{d\varphi}{1-\sin^2\alpha\,\sin^2\varphi}; \quad \overline{E} = \int_0^{\pi/2}\sqrt{1-\sin^2\alpha\,\sin^2\varphi}\,d\varphi$$

$$\overline{F}(\Gamma) = \int_0^{\Gamma}\frac{d\varphi}{\sqrt{1-\sin^2\alpha\,\sin^2\varphi}}; \quad \overline{E}(\Gamma) = \int_0^{\Gamma}\sqrt{1-\sin^2\alpha\,\sin^2\varphi}\,d\varphi$$

$$\tan\Gamma = \frac{1}{\tan\theta\,\cos\alpha}.$$

For the calculation of the forces acting on the valve head, a method is employed which is similar to that for the calculation of r and h. According to Bernouilli's theorem, we ob-

tain for the difference in pressure between a point below and a point above the valve head, $\Delta p = \frac{\gamma}{2g}(1 - w^2)$. The total pressure is then given by the integration

$$P' = \frac{\gamma}{2g}\frac{1}{b}\int (1 - w^2)\, ds,$$

whereby the factor $1/b$ must be added for a reason already mentioned. The first summand is $m + 1$, while the second part leads to the integral

$$P^* = \frac{1}{b}\int \left\{ \frac{f\cos\alpha}{f^2-1} + \sqrt{\frac{1 - f^2\sin^2}{f^2-1}} \right\} \frac{1}{f + fa}\, df$$

The calculation gives:

$$P^* = \frac{\kappa}{\pi}\cos\alpha \log\left(\operatorname{cotan}\frac{\alpha}{2}\right) - \frac{1-\kappa^2}{2\pi}\arccos\frac{fa - \sin\alpha}{1 - fa\sin\alpha}$$

$$+ \frac{\kappa}{2}\sin\alpha + \frac{1 - 3\kappa^2}{4} - \frac{\kappa\, fa}{\pi\sin\theta\cos\theta}\left\{\frac{\pi}{2} + (F-E)F(\theta,k') - F\,E(\theta,k')\right\}$$

$$\underline{+ \cos\alpha \log\frac{1-\cos\alpha}{\sin\alpha} + \log\frac{1}{\sin\alpha} + \sin\alpha\left(F - \frac{\pi}{2}\right)}$$

the underlined terms dropping out for flow IIb.

For flow I the calculation of the forces is considerably simpler, since it can be made according to the law of momentum. The forces acting on r are composed of:

1. The pressure difference

$$b\frac{\gamma}{2g}(1 - \kappa^2),$$

to infinity on both sides for the width b;

2. The deflection pressure $(\kappa - \sin\alpha)\,\pi\frac{\gamma}{g}$, since π is volume

flowing through per unit of time.

In order to obtain again nondimensional coefficients in accord with the previous researches, we further expand this with $1/b$ and obtain

$$P = \frac{1 - \kappa^2}{2} + \kappa(\kappa - \sin\alpha) \text{ (omitting } \frac{\gamma}{g}\text{)}.$$

3. Combining the results.- The values of n, m and p must now be calculated in terms of κ and α, whereby it must be borne in mind that the equations for m and n can be solved only in conjunction and that only their solution accurately determines the flow. If we then take from these equations the corresponding values of κ and α and introduce them into P, we thus obtain the value of P. The rather complicated form in which P, n, m are combined with κ and α, necessitates rather troublesome graphic and mathematical evaluations, whose results are represented in curves, with P_{IIa}, P_{IIb}, m_{IIa}, m_{IIb}, n_{IIa} and n_{IIb} as ordinates and α as the abscissa. Herein the curves κ = constant for $\kappa = 0, 0.1 \ldots\ldots 1$ were introduced (Figs. 17-23).

From the curves for m, it is immediately obvious that the whole flow in the cases IIa and IIb is confined to relatively small angles. In IIb the angles are about twice as large as in IIa. The sets of curves for h and n show, in case IIb, that for small angles, the valve lift is almost independent of α and κ, while this is not so much the case in IIa. The latter curves hold good in the region down to about

20°, since, from there down, a term appears which was neglected in the calculation.

It is easily seen that the flow in the limiting cases is in order. For large overlappings the angle is very small and finally becomes $\alpha = 90^\circ$, at $m = \infty$. At $m = 1$ (i.e., in the case where the channel is wide open), it is easily seen from the equations for m, that $\kappa = 1$ and $\alpha = 90^\circ$. In constant overlappings, κ also increases with increasing α, so that α reaches its apparent maximum at $\kappa = 1$. For positive overlappings, the maximum angle is $\alpha_{max} = 14^\circ$ in case IIb and $\alpha_{max} = 8^\circ$ in IIa. Each overlapping attains a maximum angle at $\kappa = 1$.

The course of m with negative overlappings is quite different from what it is with positive overlappings. The individual curves alternately cross one another so that, with increasing κ, α first increases, reaches a maximum and then sinks again to $\kappa = 1$. As to whether such a flow actually exists, cannot be maintained without further investigation. Since this somewhat resembles the behavior of a throttle valve, but does not concern valve flows, it was not investigated further.

In what follows, the quantities in question were determined for several overlappings. Since the valves in use show overlappings of $m = 0$-0.6, there were investigated: $m = 0$; 0.05; 0.1; 0.2; 0.3; 0.6. The corresponding values of κ, α, etc., are obtained in the following manner. In the m diagram, for

m = constant, a line is drawn parallel to the α axis. This line intersects the curve at points, each of which determines two values κ and α. These points are now introduced into the h diagrams and thus the course of the valve lift is plotted against α. Hence the result is the same here as in the case treated in Section 1. We obtain, for constant overlappings, a diagram of a set of three values of α, κ and h. From the h curves, it is obvious that they run very closely in proportion with α and κ.

The angles of deflection α of the flow is very small in both IIa and IIb. The m diagrams exhibit, for the customary overlappings, values up to α equals about 10°. All the remaining problems with regard to the different kinds of flow can be solved with the aid of the computed curves. A knowledge of the distance EE' is also important for the flow IIb. This distance must be determined again by integration. The following modification of EE' occurs with the valve lift. EE' = ∞ for $n = 0$; EE' decreases, as h increases, reaches a minimum and then increases again. It is easy to determine that, from the minimum on, there is a flow against pressure. The fact is mathematically important that the variability of EE' demonstrates that a flow, in which EE' is obtained by construction, does not necessarily exist.

4. Distinguishing between the two kinds of flow.- After the three flows have been successfully calculated from all sides,

there arises the important questions as to which kind of flow occurs in a given instance, whether there are circumstances under which two different kinds of flow can occur, etc. For small overlappings, the forces for case I show a slight decrease, but then a gradual increase with the valve lift. For greater overlappings, the forces increase continuously, though very slowly. Cases IIa and IIb (Figs. 21-22) exhibit great similarities. The forces decrease very rapidly, reach a minimum at $n = 1$ (about) and then increase rapidly. It is now necessary to consider the equilibrium of a valve head actuated by a spring. The power curve of the spring is always an ascending line. Equilibrium occurs at the point where the power curve of the spring intersects the pressure curve. There are two possible cases. Either the power of the spring decreases faster than the pressure or vice versa. Only the former case is stable, since the disturbance of the equilibrium there generates forces which tend to restore the original condition (Fig. 24). In this sense, it is easily recognized that the flows IIa and IIb are stable under all conditions down to the minimum, beyond which no definite statement can, however, be made. The flat course of the forces in case I (Fig. 23) demonstrates that the flow is to be considered stable throughout. It is easily understood that only the flows II can occur at small valve lifts, because of the otherwise very great velocities. Other conditions will, however, arise, if the valve head is held rigidly and given no freedom of motion, an arrangement on which were based the exper-

iments recently performed by Schrenk in Darmstadt. He observed the noteworthy phenomenon that, on lifting the valve head, flow II occurred first and then changed suddenly to flow I.

It is a question as to what the physical reason is for the fact that, with a certain valve lift, instability occurs when there is no spring, as in Schrenk's arrangement. It is not to be assumed that the course of the forces acting on the valve head, as stated above, has any effect on this phenomenon, although the minimum force at a valve lift is of the same order of magnitude as that of Schrenk in the rough calculation of the flow.

It is more probable that the friction on the stationary wall is responsible for this phenomenon. From the point E on, the velocity along the wall decreases from $n = \infty$ to $n = 1$ in infinity. In an actual fluid, the flow along a stationary wall is such that, as a result of the friction, the fluid adheres to the wall and the velocity then gradually increases up to the value which follows from the potential flow. The layer in which this increase occurs is very thin and is called the boundary or marginal layer. If, as in the above case, the fluid flows along a wall with increasing velocity, then the particles in the boundary layer come to rest much sooner than the more distant ones. The pressure increase therefore takes place much more quickly in the boundary layer. A point is finally reached where the pressure in the boundary layer even generates a counter-current. In most cases, the

flow then detaches itself, a phenomenon which is known from the diffuser. Similar relations also exist here. It is interesting that the points of the detachment of the Schrenk flow, plotted to scale, lie approximately in a straight line at an angle of 25°. It is therefore very natural, in connection with the Schrenk flow, to think of a diffuser in which the flow detaches itself. It is very difficult to treat this problem mathematically. We can determine approximately the course of the velocity along the horizontal wall and find a dependence according to the -1/3 power, on account of the flow at an angle of 90°. It is, however, doubtful as to whether the pressure changes with the velocity and finally becomes $-\infty$ in the angle. For this case, the methods of the Prandtl theory of a boundary layer fail completely, because they assume a constant pressure.

Translation by Dwight M. Miner,
National Advisory Committee
for Aeronautics.

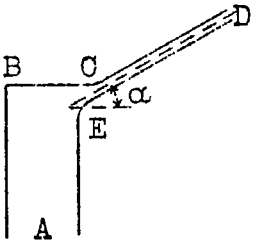

Fig.1

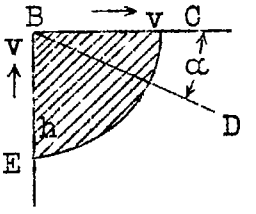

Fig.2

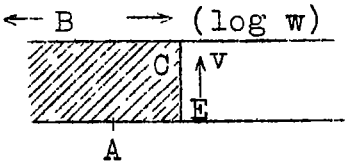

Fig.3

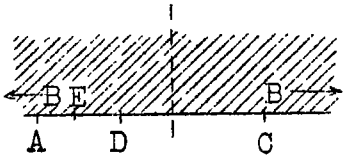

Fig.4

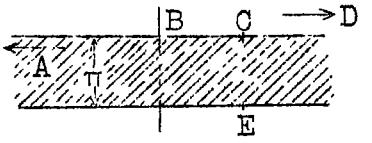

Fig.5

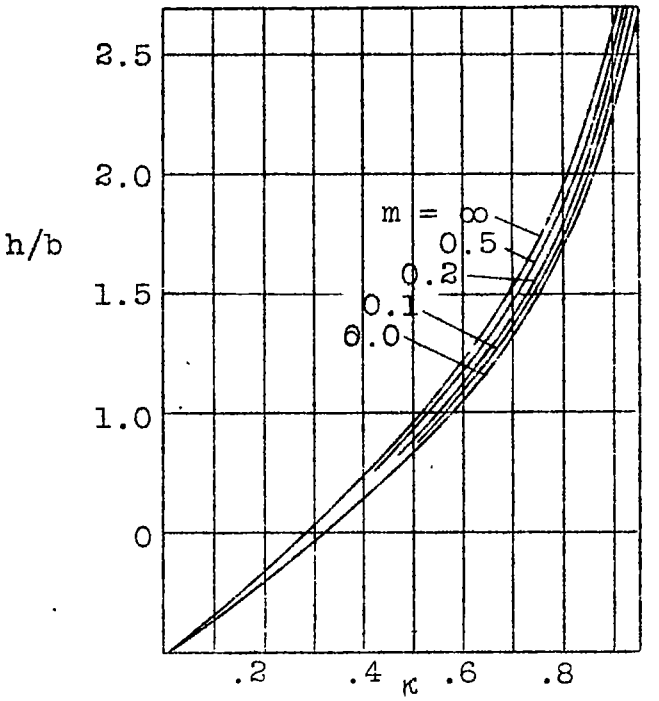

Fig.6 Velocity against the valve lift.

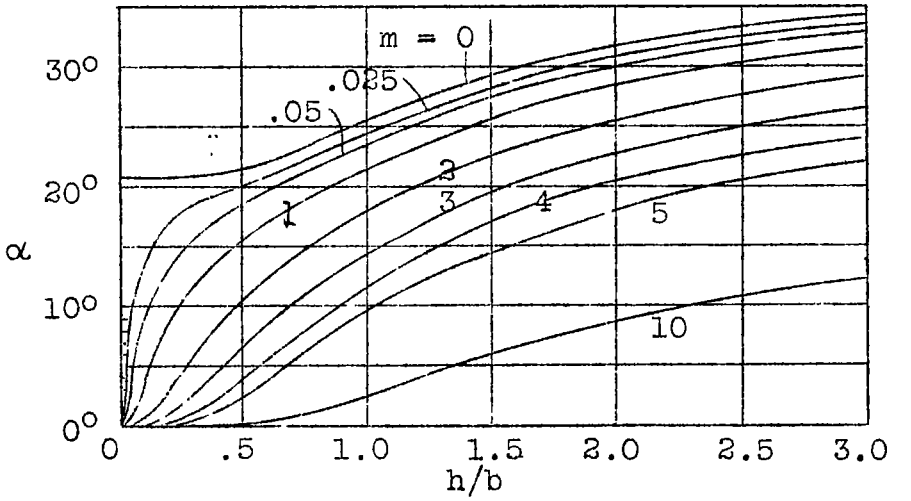

Fig.7 Angle of deflection of flow I against the valve lift

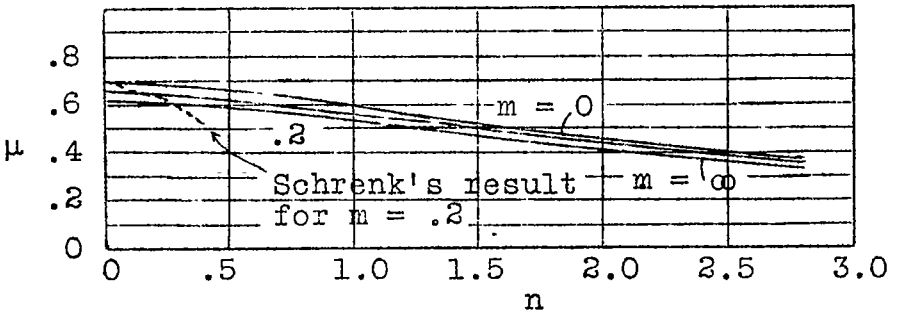

Fig.8 Coefficient of contraction $\mu = k/m$ against n

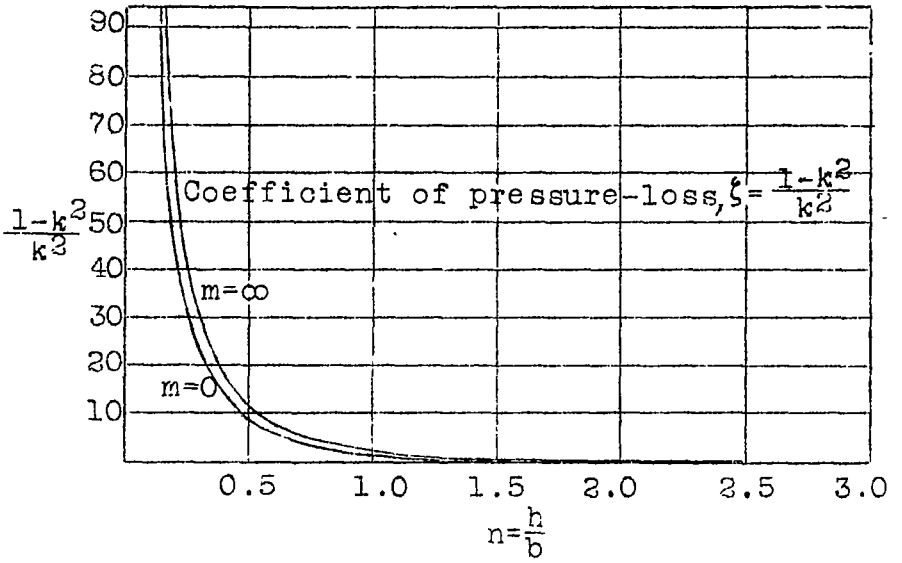

Fig.9

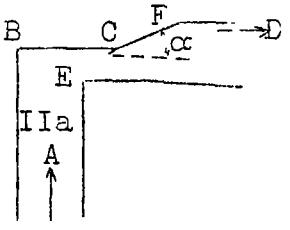

Fig.10

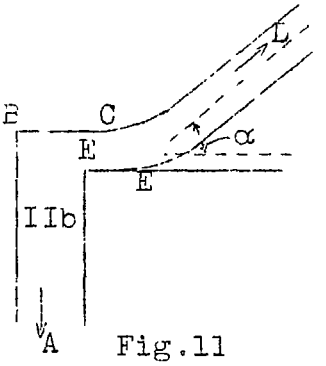

Fig.11

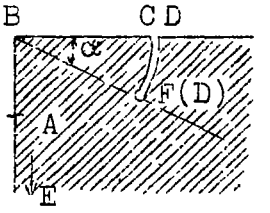

Fig.12

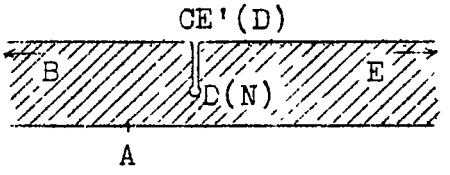

Fig.13

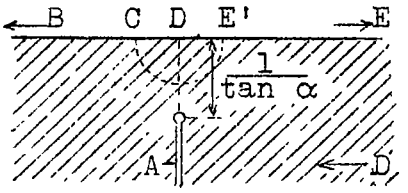

Fig.14

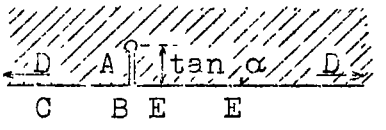

Fig.15

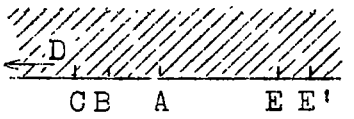

Fig.16

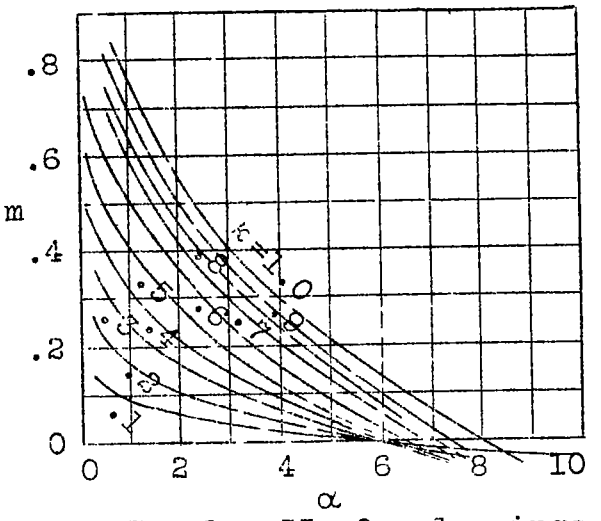

Fig.17 Flow IIa. Overlappings (m) plotted against α

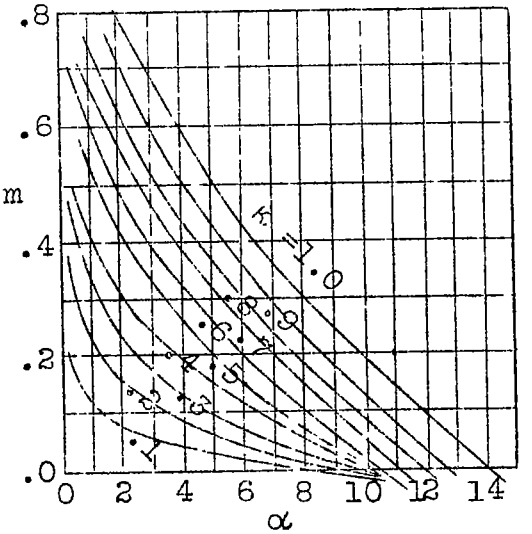

Fig.18 Flow IIb. Overlappings (m) plotted against α

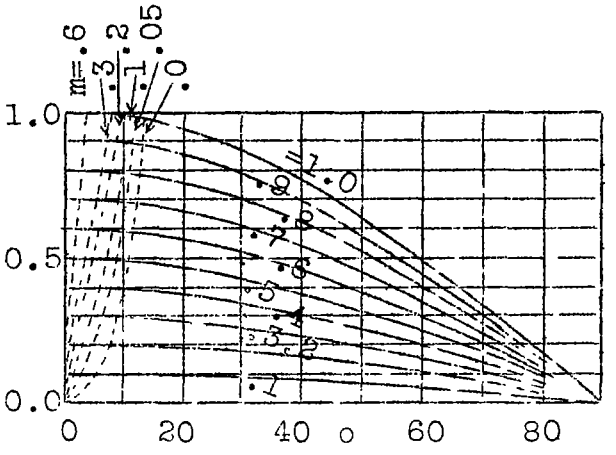

Fig.19 Flow IIb. Valve lift plotted against angle o

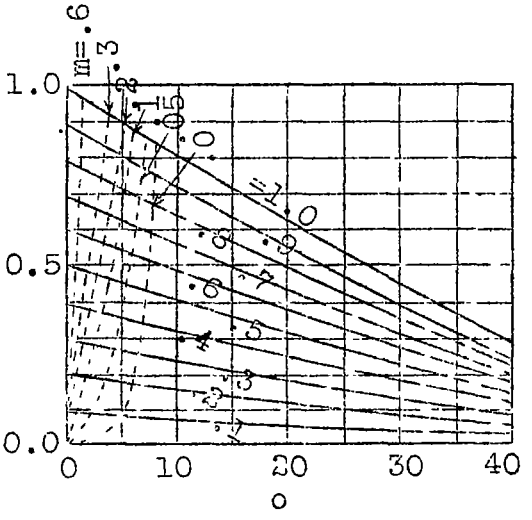

Fig.20 Flow IIa. Valve lift plotted against angle o

$$P' = 1/b \int_0^r (1-w^2)ds$$

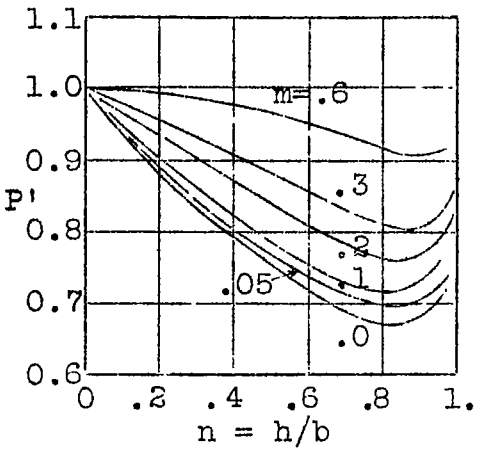

Fig.21 Flow IIb. P' plotted against valve lift.

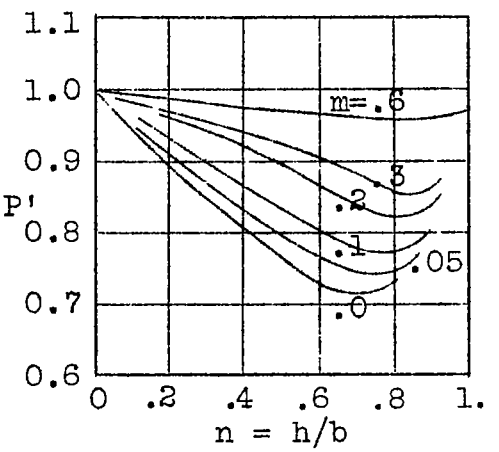

Fig.22 Flow IIa. P' plotted against valve lift.

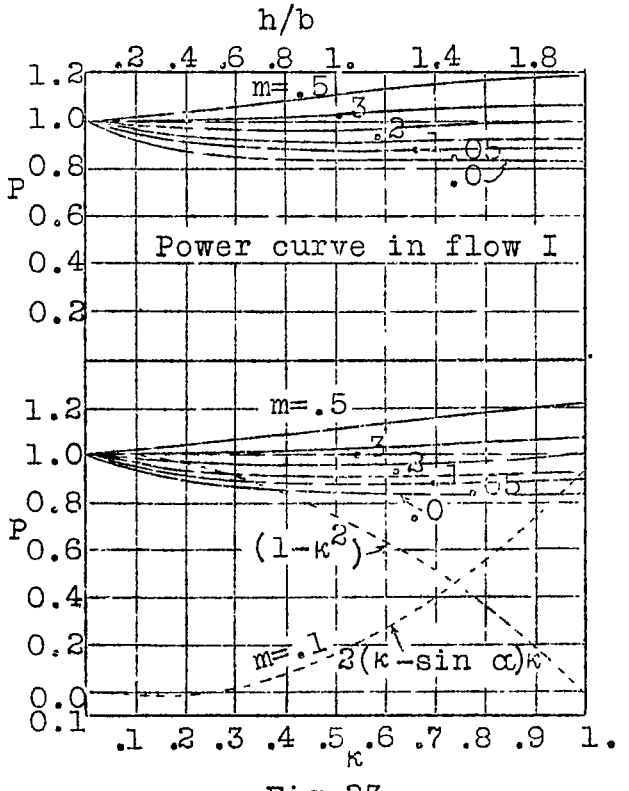

Fig.23

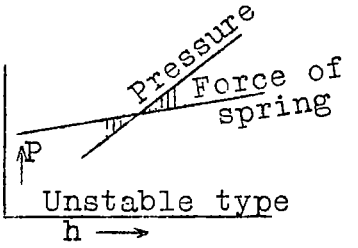

Fig.24

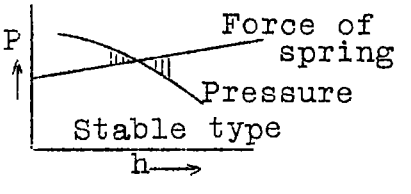

Fig.25